

Photocurable Itaconic Acid-Functionalized Star Polycaprolactone in Bio-Based Formulations for Vat Photopolymerization

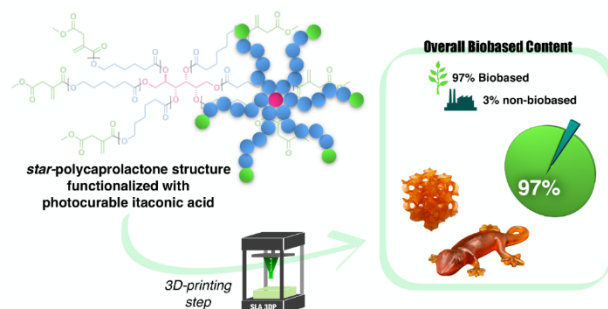
Chiara Spanu, Erica Locatelli, Letizia Sambri, Mauro Comes Franchini and Mirko Maturi†**

Department of Industrial Chemistry “Toso Montanari”, University of Bologna, Via P. Gobetti
85, 40129 Bologna (Italy)

KEYWORDS

Polycaprolactone; itaconic acid; Vat photopolymerization; biobased materials; additive manufacturing

TOC GRAPHICS



ABSTRACT

Photopolymerization-based 3D-printing techniques, such as stereolithography (SLA), are becoming more popular due to their ability to create complex geometries and material properties that are difficult to achieve with other methods. However, a major issue with photopolymerization-based techniques is that they rely on the use of harmful (meth)acrylic acid esters derived from fossil fuels. To address this, researchers have been exploring the use of biobased alternatives, such as itaconic acid, which is a building block obtained through fermentation and has a photocurable double bond. Additionally, aliphatic polyesters, such as polycaprolactone (PCL) and its hyperbranched star-like polymers, have been discovered to be biodegradable, low cost, and have intricate 3D-structures. However, their solid thermoplastic features make them unsuitable for vat photopolymerization-based techniques. This study proposes the one-pot synthesis of a liquid itaconic acid-functionalized branched polycaprolactone macromer, named sorbitol hexa(pentacaprolactone methylitaconate, SH(PCI)). The synthesized (meth)acrylic-free low molecular weight polymer was then used to create photocurable resins that could be 3D-printed into biobased thermosets with high resolution and printability. The polymer and the printed object were tested and characterized for structural, mechanical, and thermal properties, and ten different resins were proposed with biobased contents of up to 97%, which are among the highest reported in the literature so far. These resins lead to printed materials that cover a broad range of mechanical properties, including elastic moduli ranging from 22.1 to 218 MPa, elongations at break from 3.9 to 20%, and tensile strengths from 3.6 to 11.6 MPa.

INTRODUCTION

Additive manufacturing (AM), also known as 3D-printing, has emerged as the most versatile and customizable object manufacturing technique in several areas, such as medical devices, automotive, aerospace and jewellery.^{1,2} During the past years, different types of 3D printers have been developed like stereolithography (SLA), selective laser sintering (SLS) and fused deposition modelling (FDM), encompassing a huge variety of materials employed, like resins, polymers, ceramics, glasses and metals.³ However, while extrusion- or powder-based technologies have already reached a significant percentage of biobased materials used, this is not so straightforward for vat photopolymerization techniques. Currently, photopolymerization-based techniques (such as stereolithography, SLA) rely on the use of petrol-based, harmful and volatile (meth)acrylates and epoxides, and therefore there is an impelling need for their replacement with greener alternatives.⁴ With the aim of improving the sustainability of SLA-based manufacturing, the bio-based building block itaconic acid is emerging, since it is industrially obtained by fermentation of sugars.⁵ Its photocurable moiety opens for the possibility of a complete replacement of acrylic and methacrylic-acid derivatives in SLA.^{6,7} Moreover, the double carboxylic functionality allows for its incorporation into photocurable polyesters and poly(ester-amides), and for the preparation of small diesters that have been recently reported as partially biobased reactive diluents.⁸⁻¹¹

Aliphatic polyesters offer great opportunities to be used in AM thanks to their low costs, tailorable structures, biodegradability, and excellent mechanical properties.¹² Amongst these, polycaprolactone (PCL) has emerged thanks to the various renewable resources available for

its production.¹³⁻¹⁵ Ring-opening polymerization (ROP) is performed for its obtainment and the monomer used is ϵ -caprolactone, which is considered a bio-based building block thanks to the various renewable resources available for its obtainment, such as lignocellulosic biomass or biotechnological sourcing.¹⁴⁻¹⁶ Only a few works have implemented it in stereolithography, with the aim of printing scaffolds for tissue regeneration or drugs release,¹⁷⁻¹⁹ while there is a single example reporting PCL macromers for SLA, but functionalized with (meth)acrylic acid and printed at temperature above the melting point of the PCL structure, thus with poor final biobased content and high energy consumption. Moreover, the described 3D-printed materials retained most of the physical-chemical properties of PCL, such as low thermal stability and fast biodegradability, that represent considerable drawbacks for structural and durable components. Given its many interesting properties, polycaprolactone has been employed even as a hyperbranched star-like polymer. These types of branched polymers have gained high attention in different fields, like coatings, drug delivery and as additives, due to low melt viscosity, higher solubility and higher functional end-groups per unit volume.²⁰ Polyalcohols, such as glycerol, trimethylolpropane, pentaerythritol and D-sorbitol, are chosen as starting sources for the star-like polymer's synthesis and depending on the different alcohols chosen, it's possible to tune the number of final arms generated.²¹ D-sorbitol, with its six terminal hydroxylic groups, represents an appealing choice for the development of a highly branched PCL polymer, that opens the possibility for an extensive subsequent modification with new end groups.

This work proposes, for the very first time, the one-pot synthesis of a low molecular weight star polycaprolactone structure functionalized with itaconic acid, and its formulation into biobased liquid resins for SLA. At first, the effect of the content of photocurable PCL macromer on the mechanical properties of methacrylate-based 3D-printed materials is explored; then, methacrylate components were replaced with biobased itaconic acid esters, allowing for the 3D-printing of crosslinked photopolymers with biobased contents as high as 97% and with mechanical properties comparable to those of commercially available fossil-based formulations.

MATERIALS AND METHODS

Monomethyl itaconic acid was prepared from cyclic itaconic anhydride as previously reported.²² Cyclic itaconic anhydride was synthesized from itaconic acid as previously described by Pérocheau et al.¹⁰ Pentaerythritol tetraacrylate (PETA) was purchased from Tokyo Chemical Industries (TCI). Tetrahydrofuran (THF) and triethylamine (TEA) were dried before use by distillation over Na-benzophenone. ϵ -caprolactone was dried over CaH_2 and freshly distilled under reduced pressure prior to use. Grindsted Soft-N-Safe (9-hydroxystearic acid monoglyceride triacetate, SNS) was purchased from Danisco (Brabrand, Denmark). 1,4-butanediyl bis(methyl itaconate) was prepared as previously described.¹¹ All other chemicals were purchased from Sigma Aldrich (Saint-Louis, MO, USA) and used as received.

Synthesis of monomethyl itaconoyl chloride

In a 1-L round-bottomed flask under nitrogen atmosphere equipped with a CaCl_2 drying tube, 180 mL of oxalyl chloride (2.1 mol) were added to itaconic acid monomethyl ester (216 g, 1.5 mol). The reaction was allowed to take place by stirring overnight at room temperature. Once the reaction was completed all the acid was dissolved, and unreacted oxalyl chloride was distilled at room temperature under high vacuum and recovered for further use. Then, the temperature was increased to 120°C and pure monomethyl itaconoyl chloride was distilled off as a colourless liquid from the reaction mixture and stored under inert atmosphere in the dark at -20°C . ^1H NMR (400 MHz, CDCl_3) δ 6.72 (s, 1H), 6.18 (s, 1H), 3.72 (s, 3H), 3.40 (s, 2H). Yield = 86%

Synthesis of sorbitol hexa(pentacaprolactone methylitaconate)

In a dry three-necked 1-L round-bottomed flask with N_2 inlet, 18.2 g of sorbitol (0.1 mol) were dispersed in 300 mL of dry anisole, and 332 mL of freshly distilled caprolactone (342 g, 3 mol)

were added under stirring using a needle. Then, a dry condenser was placed on one of the necks, 5.84 ml of Sn(oct)₂ were added and the mixture was stirred under reflux (oil bath at 180°C) for 4 h. Then, the mixture was cooled to 0°C with an ice bath and 85 mL of dry triethylamine (TEA, 0.61 mol) were added with a syringe, followed by the dropwise addition of 80 mL of monomethyl itaconoyl chloride (0.61 mol) taking care to keep the temperature of the mixture below 10°C. The reaction was allowed to take place by stirring overnight at room temperature. The next day, TEA salts were precipitated by adding around 300 mL of THF, the mixture was filtered to remove the salts and THF was evaporated under vacuum. Then, the polymer was purified by washing with cold methanol, which caused the polymer to separate at the bottom as a denser liquid. The process was repeated three times, then the residual anisole is removed by adding some water and removing it by rotavapor. The final product is collected as a viscous liquid. Yield = 72%

Synthesis of dodecyl methylitaconate (DOIT) and 1,4-butanediyl mono(methylitaconate) (Me-MONO)

In a dry 1-L round-bottomed flask equipped with a magnetic stirrer and nitrogen inlet, 1-dodecanol (0.8 mol, 180 mL) or 1,4-butanediol (0.8 mol, 72.1 g) was mixed with 500 mL of dry THF or anisole, followed by the addition of 112 mL (0.8 mol) of dry triethylamine (TEA). The mixture was cooled to 0°C using an ice bath, and then monomethyl itaconoyl chloride (100 mL, 0.8 mol) was slowly added dropwise. At the end of the addition, the ice bath was removed, and the mixture was stirred at room temperature for 2 hours. Then, 500 mL of water were added to dissolve TEA salts and the organic solvent was removed by rotary evaporation. The organic phase was extracted three times using ethyl acetate, the collected organic phases were dried over sodium sulfate and evaporated to afford DOIT as a yellow-to-red liquid. For DOIT: Yield = 84%. ¹H-NMR (400 MHz, CDCl₃) δ 6.32 (s, 1H), 5.69 (s, 1H), 4.15 (t, 2H), 3.69 (s, 3H), 3.34 (s, 2H), 1.65 (m, 2H),

1.28 (m, 18H), 0.88 (t, 3H). ESI-MS: $[M+Na^+] = 335$. For Me-MONO: Yield = 87%. 1H -NMR (400 MHz, $CDCl_3$) δ 6.33 (s, 1H), 5.71 (s, 1H), 4.20 (t, 2H), 3.70 (5H), 3.34 (s, 2H), 1.77 (m, 2H), 1.64 (m, 2H). ESI-MS: $[M+Na^+] = 239$.

Synthesis of poly(dodecanediyl itaconate) oligomer (oligoPDI)

In a 1-L round bottomed flask, dimethyl itaconate (474 g, 3 mol) and 1,12-dodecanediol (404 g, 2 mol) are mixed with 5.25 g (21 mmol) of dibutyltin (IV) oxide. The mixture was heated to 150°C for 1 h during which the methanol produced by the transesterification reaction was removed by distillation. At the end of the reaction, the mixture was cooled to room temperature, dissolved in ethyl acetate and washed with water for 3 times. The organic phase was therefore dried over sodium sulfate and evaporated to afford oligoPDI as a waxy solid with a melting point around 30-40°C. Yield = 91%. 1H -NMR (400 MHz, $CDCl_3$) δ 6.28 (3H), 5.67 (3H), 4.12 (t, 4H), 4.05 (t, 4H), 3.74 (s, 3H), 3.66 (s, 3H), 3.30 (6H), 1.60 (m, 8H), 1.25 (32H). ESI-MS: $[M+Na^+] = 773$.

Formulation and 3D printing

For the formulation of the photocurable resins, SH(PCI) and the co-monomers were placed in a 150 mL plastic container according to the weight percentages reported in Table 1. Typically, 100 g of each resin were prepared, and therefore the weighted amount of each component (in grams) is numerically equivalent to the weight percentages reported in the table. To these mixtures, the photoinitiating system composed of 1.7 g of ethyl phenyl (2,4,6-trimethylbenzoyl) phosphinate (Et-APO), 1 g of methyl hydroquinone (MHQ), and 300 mg of 2-isopropyl thioxanthone were added to all formulations. The mixtures were homogenized using a fix-speed planetary mixer (Precifluid P-MIX100) for 3 minutes. Once formulated, the resins were poured into the vat of a Phrozen Sonic 4K stereolithographic 3D printer working with a 6.1 inches 50 W monochrome 405 nm ParaLED Matrix 3 UV screen (3840x2160 resolution, 4K) and printed into specimen for

mechanical tests or other 3D objects. The g-codes used by the printer for the process were generated using the slicer software Chitubox Basic 1.9.4 with a layer height of 100 μm and an exposure time per layer of 100 s. All prints were performed at 25°C. For tensile tests, dog-bones were printed according to the ISO 37 Type 2 ($75 \times 12.5 \times 2 \text{ mm}^3$) specifications. Once printed, all samples were gently detached from the building plate and rinsed in an acetone-isopropanol (1:1) mixture to eliminate the non-polymerized resin. Then, the raw 3D printed objects were post-cured for 20 min at room temperature in a UV chamber (Sharebot CURE, wavelength 375–470 nm, 34.7 mW/cm^2) to ensure complete polymerization of itaconate and methacrylate units.

Materials Characterization

^1H and ^{13}C NMR spectra were obtained on Varian Inova (14.09 T, 600 MHz) and Varian Mercury (9.39 T, 400 MHz) NMR spectrometers. In all recorded spectra, chemical shifts have been reported in ppm of frequency relative to the residual solvent signals for both nuclei (^1H : 7.26 ppm and ^{13}C : 77.16 ppm for CDCl_3). ^{13}C NMR analysis was performed using the ^1H broad band decoupling mode. Mass spectra were recorded on a micromass LCT spectrometer using electrospray (ES) ionization techniques. ATR-FTIR analysis has been performed using a Cary 630 FTIR spectrometer (Agilent). Rotational viscosity measurements were performed on an Anton Paar MCR102 modular compact rheometer with a CP50–1 geometry, indicating a plate-cone geometry with 1° angle and diameter of 25 mm, with a constant rotational frequency of 1 Hz. Size exclusion chromatography (SEC)/gel permeation chromatography (GPC) was performed on a Knauer system (controlling a Smartline Pump 1000 equipped with a K-2301 refractive index detector). A Shimadzu Shim-Pack GPC-803 column ($0.8 \text{ cm} \times 30 \text{ cm}$) and a Shimadzu Shim-Pack GPC-800P ($10.0 \times 4.6 \text{ mm}$) guard column were used as column systems. HPLC-grade tetrahydrofuran (THF) was used as the eluent with a flow rate of 1 mL/min . The system was calibrated with polystyrene

(PS) standards obtained from linear PS covering a molar mass range from 750 to 20000 g/mol (Merck). Thermogravimetric analysis (TGA, Netzsch TG 209 F1 Libra) was carried out in a nitrogen atmosphere by heating the sample (10–15 mg) at a rate of 20 °C/ min from 30 to 700 °C in a platinum crucible. Then, the inert atmosphere was replaced with air to evaluate the inorganic residue after the 30 min isothermal step. Differential scanning calorimetry (DSC) measurements were carried out on a TA Instruments Q2000 DSC modulated apparatus equipped with a refrigerated cooling system (RCS). Samples (10–15 mg) were heated from –88 to 150 °C at 20 °C/min in standard nonhermetic aluminum pans. A Remet TC10 universal testing machine was used to perform all the tensile tests. The instrument was equipped with a 10 N cell, with a crosshead separation speed of 1 mm min⁻¹ according to the ISO 37 Type 2 specifications.

RESULTS AND DISCUSSION

Sorbitol hexa(pentacaprolactone methylitaconate) SH(PCI) was prepared by $\text{Sn}(\text{oct})_2$ -catalyzed ring-opening polymerization (ROP) of ϵ -caprolactone using D-sorbitol as the polymerization initiator, followed by functionalization with monomethyl itaconoyl chloride (MIC) without any intermediate step of purification (**Figure 1**). Anisole was selected as ROP solvent thanks to its sustainable production and use, and its high boiling point.²³ The caprolactone/OH molar ratio was set to five, which was expected to produce a branched polymer that could be liquid at room temperature. The nature of the ROP mixture allowed for proceeding with the acylation of the terminal groups of PCL without the occurrence of side reactions.

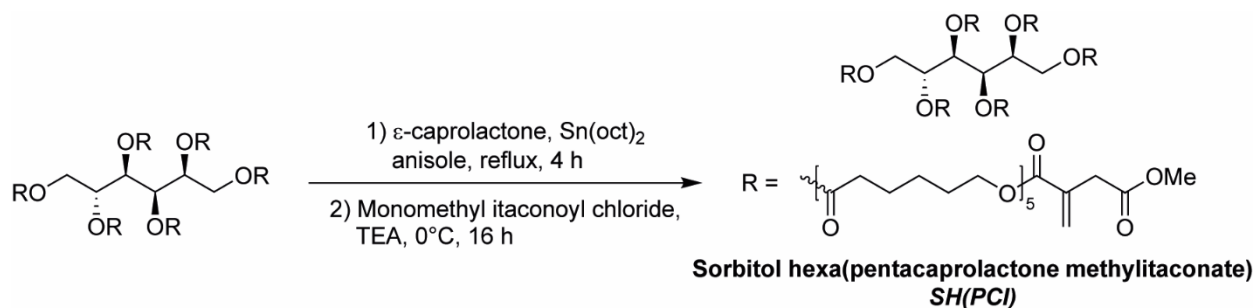


Figure 1. Reaction scheme for the one-pot synthesis of sorbitol hexa(pentacaprolactone methylitaconate)

The product was characterized by means of 1D- and 2D-NMR spectroscopy (**Figure 2a** and **Figure S1-S3**). MIC was prepared by chlorination of the carboxylic acid obtained by

methanolysis of itaconic anhydride, leading to the preferential formation of the α,β -unsaturated acyl chloride (**Figure S4**). However, smaller amounts of the inverse compound, the α,β -unsaturated methyl ester, were also formed but could not be separated by distillation due to their similar boiling points. This is reflected in the NMR spectra of SH(PCI), where signals related to atoms close to the carboxylic functionalities of itaconic acid are split due to the presence of itaconate units in both orientations. In the ^1H -NMR spectrum of SH(PCI), such splitting is not only observed for the singlet signal of the methyl ester group (3.67 and 3.75 ppm), but also for the alcoholic CH_2 group of caprolactone units (4.03 and 4.14 ppm), suggesting the presence of itaconic acid moieties at the end of PCL chains.

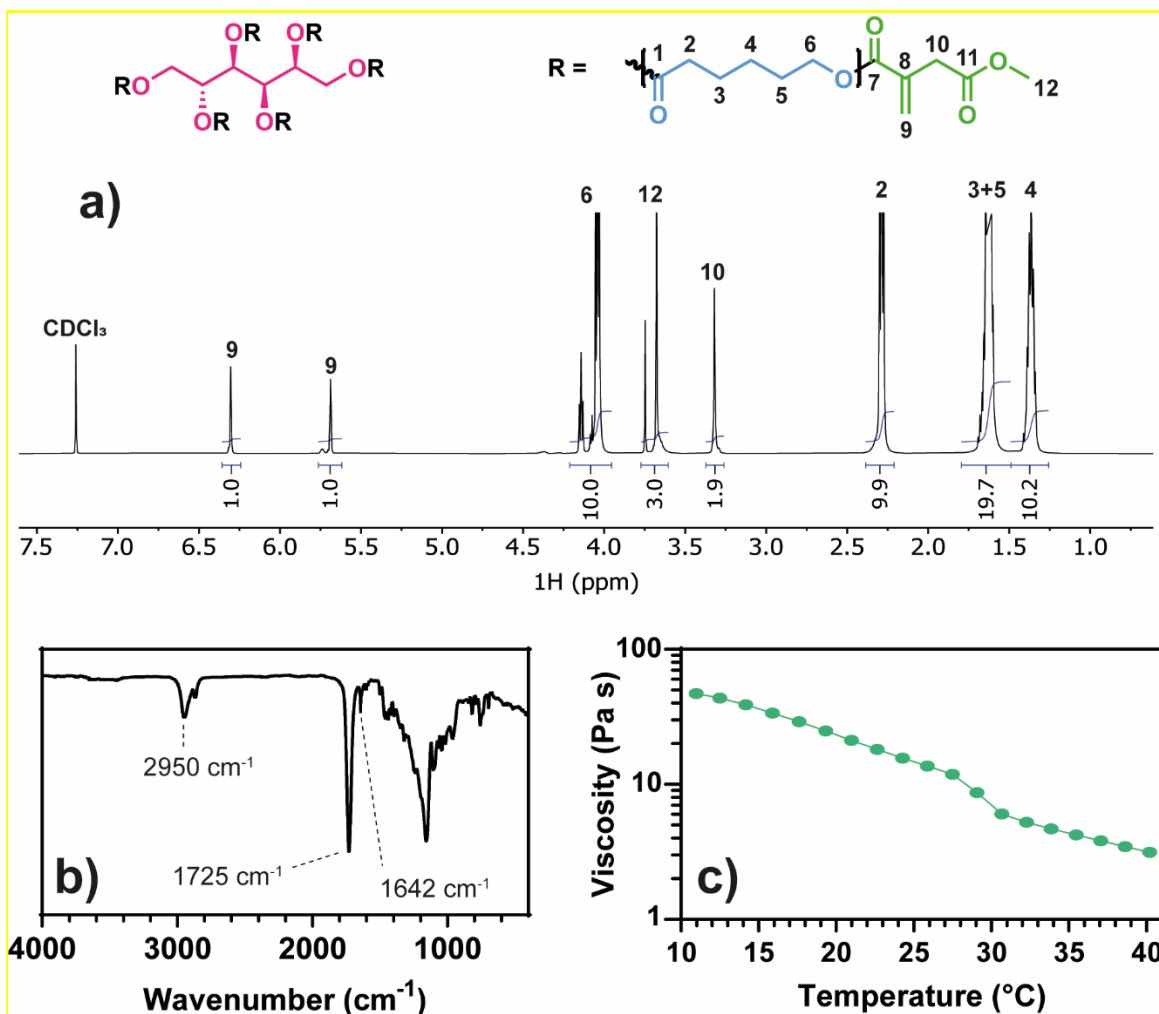


Figure 2. Characterization of sorbitol hexa(pentacaprolactone methylitaconate). a) ¹H-NMR spectrum (CDCl₃, 400 MHz) of SH(PCI) and the corresponding spectral assignments. c) ATR-FTIR spectrum. d) Viscosity of SH(PCI) as a function of temperature, measured at constant shear rate (1 Hz). Error bars are not shown because they are smaller than the data point symbol. This is also supported by the absence of a signal of non-esterified alcoholic CH₂ of caprolactone, which would have been expected as a triplet around 3.5 ppm.²⁴ Therefore, the one-pot polymerization-esterification of pentacaprolactone itaconate on sorbitol has proven to be efficient end quantitative. Furthermore, by comparing the NMR integrals of peak 6 (alcoholic CH₂ of caprolactone monomers) and peak 9 (methylene group of itaconic acid) and assuming

that itaconic acid units are present at the end of PCL chains, it is possible to calculate the average number of caprolactone units per arm as equal to 5. Due to their low abundance, sorbitol core units could not be observed in the NMR spectrum at the same scale as the signals arising from PCL or itaconate units, but by zooming in the HSQC spectrum of the compound, it was possible to identify its presence in the macromolecules (**Figure S5**). Thanks to the phase-sensitivity of the HSQC experiment, it was possible to identify and distinguish the CH and CH₂ signals of sorbitol, even though the close proximity of the former with one of the very intense PCL peaks makes it difficult to indicate an isolated cross-peak.

GPC-SEC (**Figure S6**) revealed a molecular weight distribution with $M_n = 5650$ and $M_w = 9000$ (PDI = 1.6), allowing to calculate an average number of caprolactone units per arm equal to 6.9. The discrepancy between the arm lengths calculated by GPC and NMR can be associated to the poor molecular resemblance of branched SH(PCI) with the linear polystyrene standards used for the calibration of the molecular weight analysis.²⁵⁻²⁷ By considering the conclusions drawn from NMR analysis, i.e. the fact that PCL arms are composed of 5 caprolactone units terminating with one itaconic acid methyl ester functionality, it is possible to calculate the theoretical number of arms of the star copolymer as depicted in **Equation 1**:

$$n = \frac{MW_{SH(PCI)} - MW_{sorbitol}}{5 \cdot MW_{CL} + MW_{MIT}} \quad \text{Equation 1}$$

Where $MW_{SH(PCI)}$ is the molecular weight of the macromer obtained by GPC analysis (equal to 5650 g/mol), $MW_{sorbitol}$ is the molecular weight of sorbitol (182 g/mol), MW_{CL} is the molecular weight of caprolactone units (114 g/mol) and MW_{MIT} is the molecular weight of

itaconic acid methyl ester (144 g/mol) and n is the number of arms of the star copolymer, therefore equal to 7.6. Since it is not reasonable to expect sorbitol to form polymers with more than 6 arms, and keeping into account the overestimation of the molecular weight that PS-calibrated GPC has previously demonstrated to provide, it is reasonable to expect that the macromers are composed of six-branched PCL star copolymer with a sorbitol core and five caprolactone units per arm, and each arm display an itaconic acid moiety at their termini.

The product was further characterized by ATR-FTIR spectroscopy (**Figure 2b**), which mainly displays the peaks corresponding to the PCL structure: in particular, the peaks associated with ester C=O stretching at 1725 cm^{-1} and the aliphatic CH₂ stretching at 2950 cm^{-1} . Moreover, the low intensity band associated with photocurable itaconate moieties (C=C stretching) can be observed at 1642 cm^{-1} .^{28,29} Finally, to evaluate the applicability of SH(PCI) as the main component of a liquid photocurable formulation for VAT photopolymerization, its viscosity was assessed, both at constant temperature over a range of different applied shear rates and over a wide range of temperature at constant shear rate (**Figure 2c** and **Figure S7**). Rheological curves reveal a constant decrease in viscosity with increasing temperature, related to the increase in macromolecular mobility. Between 27.5 and 30°C viscosity decreases faster, rapidly recovering the initial decrease rate with increasing temperature. This effect might be associated with the melting of SH(PCI) taking place in this range of temperature, which causes the transition to a lower set of viscosity values. This is coherent with what was previously reported from sorbitol-initiated branched PCL structures, that displayed melting temperatures around 30-45°C.¹⁶ Anyways, SH(PCI) display viscosity values compatible with the formulation

of photocurable resins for stereolithography throughout the entire range of temperatures, especially above 20°C. Moreover, the linear relationship between shear stress and shear rate in experiments performed at constant temperatures reveal the Newtonian behaviour of SH(PCI), as well as the negligible dependence of viscosity on the shear rate.

Differential scanning calorimetry (**Figure S8a**) was employed to assess the thermal behaviour of SH(PCI), revealing an endothermic peak in the 25-35°C interval, which is consistent with the reduction in polymer viscosity detected in that range. Furthermore, thermogravimetric analysis (**Figure S8b**) was employed to assess the temperature stability of SH(PCI), revealing negligible degradation up to 250°C.

Additionally, itaconic acid-based photocurable liquids have been synthesized to be employed as mono- or multifunctional reactive diluents in the formulations (**Figure 3**).

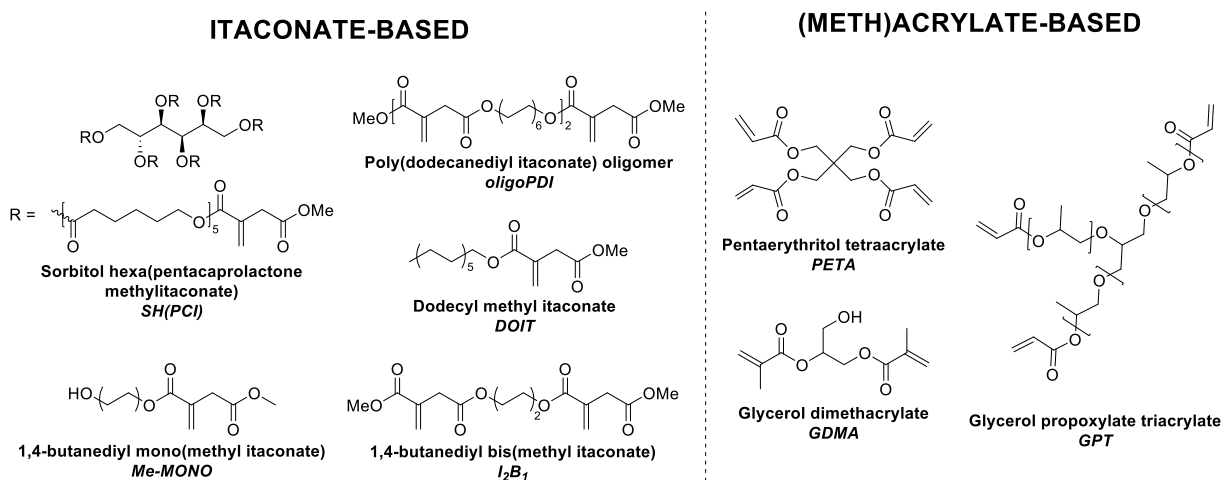


Figure 3. Chemical structures of the employed itaconate- and (meth)acrylate-based reactive diluents.

As monofunctional components, Me-MONO (mono(1,4-butanediyl) methyl itaconate, **Figure S9**) and DOIT (dodecyl methyl itaconate, **Figure S10**) were synthesized; as multifunctional components I₂B₁ (butanediyl bis(methyl itaconate)) and oligoPDI (poly(dodecanediyl itaconate) oligomer, **Figure S11**) were prepared. While the firsts were prepared by reaction of MIC with 1,4-butanediol and 1-dodecanediol, respectively, the rest were prepared by transesterification of dimethyl itaconate with 1,4-butanediol and 1,12-dodecanediol, respectively, adjusting the molar ratios to achieve the desired molecular weights. In addition to the synthesized itaconic acid-based reactive diluents, commercially available (meth)acrylate crosslinking agents such as pentaerythritol tetraacrylate (PETA), glycerol dimethacrylate (GDMA) and glycerol propoxylate triacrylate (GPT, M_n = 478) were employed (**Figure 2**). The branched polyester SH(PCI) was then formulated in different proportions with the reactive diluents, to achieve the compositions summarized in **Table 1**. To all formulations were added the biobased plasticizer derived from castor oil (9-hydroxystearic acid monoglyceride triacetate, Grindsted Soft-N-Safe, SNS, 7 wt.%), a photoradical initiator (ethyl phenyl (2,4,6-trimethylbenzoyl) phosphinate, Et-APO, 1.7 wt.%), a UV photo absorber (2-isopropylthioxantone, ITX, 0.3 wt.%) and a radical inhibitor (methyl hydroquinone, MHQ, 1 wt.%).

	SH(PCI)	DOIT	oligoPDI	Me-MONO	LB ₁	PETA	GDMA	GPT	Resin Viscosity at 25°C	Overall biobased content	Elastic Modulus ^a (MPa)	Elongation at Break ^a (%)	Tensile Strength ^a (MPa)
A1	20%	30%	30%	-	-	10%	-	-	0.55	87%	116 ± 6	3.9 ± 0.6	3.9 ± 0.5
A2	40%	20%	20%	-	-	10%	-	-	0.92	87%	82.1 ± 6.2	9.2 ± 1.8	6.5 ± 1.1
A3	50%	20%	20%	-	-	-	-	-	1.2	97%	22.1 ± 2.0	20.0 ± 2.9	3.6 ± 0.4
B1	40%	-	-	20%	20%	10%	-	-	0.88	87%	157 ± 4	10.8 ± 1.1	10.7 ± 0.5
B2	50%	-	-	15%	15%	10%	-	-	1.1	87%	78.2 ± 5.4	17.6 ± 3.5	7.4 ± 0.9
B3	50%	-	15%	15%	-	10%	-	-	1.2	87%	76.0 ± 3.1	15.1 ± 1.0	7.7 ± 0.3
G0	0%	-	-	-	-	-	45%	45%	0.34	29%	1251 ± 69	1.0 ± 0.3	12.1 ± 3.1
G1	18%	-	-	-	-	-	36%	36%	0.55	43%	503 ± 60	1.6 ± 0.7	7.4 ± 3.7
G2	40%	-	-	-	-	-	25%	25%	1.1	59%	218 ± 16	8.0 ± 1.9	11.6 ± 1.6
G3	72%						9%	9%	3.1	84%	41.9 ± 1.7	18.4 ± 2.4	5.2 ± 0.5

^a Data are expressed as mean ± SD, obtained on 5 replicate measurements for each tested material.

Table 1. Weight composition of the tested formulations for stereolithography, their corresponding biobased content, calculated as the overall mass in the system coming from sustainable resources (as wt.%), and tensile properties of 3D-printed formulations. Resins compositions sum up to 90 wt.% because the remaining 10 wt.% is composed by the plasticizer (SNS, 7 wt.%) and the photoinitiating system (Et-APO 1.7 wt.%, ITX 0.3 wt.% and MHQ 1 wt.%).

The biobased content of each formulation was evaluated by considering for each of the components, the percentage of their molecular weight that is composed of renewable and sustainable building blocks. In addition to itaconic acid and caprolactone, whose sustainable derivation was commented in the Introduction section, we considered as fully biobased also 1,4-butanediol (widely produced from biomass³⁰), sorbitol (produced by decomposition and reduction of naturally occurring polysaccharides³¹), 1,12-dodecanediol (biotechnologically produced from engineered bacteria, and by hydrogenation of biobased 1,12-dodecanedioic acid³²), 1-dodecanol (prepared by reduction of lauric acid extracted from coconut oil³³), glycerol (obtained by hydrolysis of triglycerides, also byproduct of biodiesel production), and 9-hydroxystearic acid monoglyceride (naturally occurring monoglyceride). Details of the calculation are available in the Supporting Information.

A first set of formulations (named A1, A2 and A3) contained increasing amounts of SH(PCI) in a system composed mainly of biobased C₁₂ chains³² (DOIT and oligoPDI), while a second set of resins (named B1, B2 and B3) was prepared using mono- and bifunctional itaconates deriving from shorter 1,4-butanediol (Me-MONO and I₂B₁). The effect of the addition of a highly reactive non-biobased crosslinker such as PETA was evaluated in both systems. Then, a rigid methacrylate-based resin composed of GDMA and GPT was printed, and the effect of the addition in the formulation of SH(PCI) was evaluated on the mechanical properties of the 3D printed material (named G0, G1, G2 and G3).

The viscosity of the formulation was measured at 25°C, showing that all compositions possess viscosities in the 0.25 – 10 Pa s, which has been reported has the optimal range for applications

in vat photopolymerization for 3D printing applications (Table 1).³⁴ All formulations underwent SLA 3D-printing to achieve solid 3D objects. The compatibility of the prepared resins with organic dyes was also tested by adding 0.005 wt.% of purpurin, which led to the manufacturing of colored 3D objects with high accuracy and resolution (Figure 4).

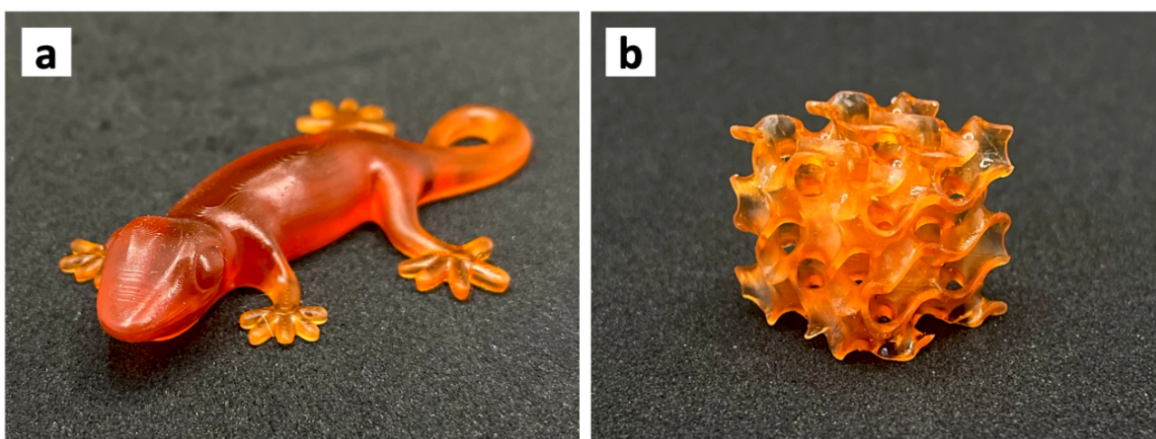


Figure 4. High-resolution 3D-printed object prepared with formulation A3 after the addition of the red dye purpurin 0.005 wt.%. Object size is a) 60x35x25 mm³ and b) 40x40x40 mm³. 3D object files obtained from www.thingiverse.com

The capability of the proposed resin to print complex architectures and geometries was evaluated successfully (Figure S12). Resin A3 was printed into a test specimen that included round structures, thin walls, sharp spikes, tilted structures and overhanging bridges, showing optimal printability, structural stability, printing accuracy and resolution.

The mechanical properties of the printed materials were evaluated by means of tensile testing on 3D-printed dog-bones. The single stress-strain curves are available in the Supporting

Information (**Figure S13** and **S14**) and the extracted results in terms of elastic modulus, elongation at break and tensile strength are summarized in **Table 1**.

By comparing the stress-strain curves of the G group of resins (**Figure 5a**), the effect of SH(PCI) is evident: as the SH(PCI) content increases, the elastic modulus decreases, while the elongation at break increases remarkably. More quantitatively, by plotting the tensile properties of the different formulations against the corresponding SH(PCI) content, a linear correlation between the PCL itaconate content and the logarithm of elastic modulus and elongation at break is evident (**Figure 5b-d**). However, there seems to be no direct correlation between the SH(PCI) content and the measured tensile strength. Nonetheless, these strict relationships allow to predict the behavior of new untested SH(PCI) contents in the GPT/GDMA 1:1 formulation, therefore making it possible to tune the elastic modulus of the desired formulation from 40 to 1250 MPa and their elongation at break from 1 to 18% just by selecting the appropriate amount of SH(PCI) to be included in the resin. Moreover, the introduction of SH(PCI) has allowed to increase the biobased content of G-resins from 29 wt.% for G0 to 84 wt.% for G3.

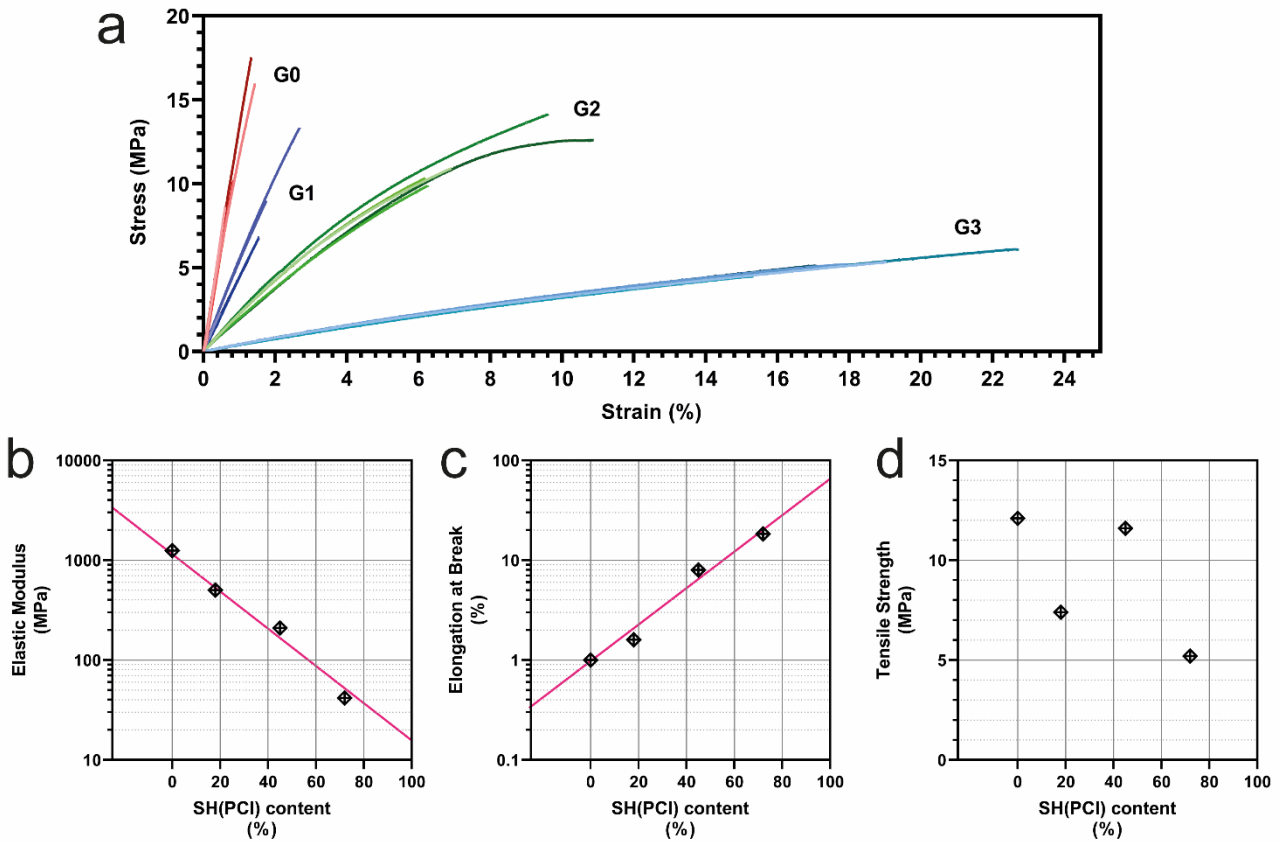


Figure 5. a) Overlap of tensile stress-strain curves for G0-G3 resins. b-d) Extracted tensile properties as a function of SH(PCI) content.

The second set of formulations (A1-A3) was prepared in order to evaluate the effect of the SH(PCI) content in itaconate-based formulations containing C₁₂ chains, with or without the presence of PETA as the acrylate crosslinker. By comparing 3D-printed formulations A1 and A2 it can be noticed that an increase in SH(PCI) content from 20% to 40% lead to a decrease in the elastic modulus, accompanied by a strong enhancement of the elongation at break, leading to an overall doubling of the tensile strength. Moreover, in the absence of PETA (formulation A3), the modulus drops as expected by the absence of the highly crosslinking

properties of the tetraacrylate, but the elongation at break doubles reaching values as high as 20%. Then, a last set of formulations (B1-B3) was tested to assess whether the effect of SH(PCI) on the performances of the 3D-printed materials was dependent on the nature of the reactive diluents. For all formulations, despite the presence of PETA, the displayed elongations at break ranged from 10% to 20%, which are remarkably high values for formulations containing 10% of a tetraacrylate crosslinker. By comparing the 3D-printed A and B formulations, it is also possible to identify the role of the itaconic acid-based reactive diluents: the presence of long C₁₂ chains have a negative effect on the materials properties, while the use of short mono- and bifunctional butanediol-based crosslinkers lead to the highest tensile strengths, without affecting too much the elastic moduli. All resins formulated in this sets (A1 to B3) have an overall biobased content as high as 87%, reaching the outstanding value of 97% for resin A3.

CONCLUSIONS

In conclusion, in this work we have reported the one-pot synthesis of biobased itaconic-acid functionalized six-branched PCL macromers (SH(PCI)) that can be formulated with (meth)acrylate- and itaconate-based reactive diluents for the high-resolution 3D-printing of biobased thermosets.³⁵ A strict correlation was observed between the mechanical properties of the printed materials and the SH(PCI) content, allowing for tuning the elastic modulus of the desired formulation from 40 to 1250 MPa and their elongation at break from 1 to 18% just by selecting the appropriate amount of SH(PCI) to be included in a methacrylate-based rigid resin. Moreover, the presented macromer has proved its compatibility with (meth)acrylate-free reactive diluents, leading to 3D-printed materials with biobased contents amongst the highest ever reported and mechanical properties that are competitive with the ones of many petrol-based commercial alternatives.

ASSOCIATED CONTENT

Supporting Information. 1D and 2D NMR analysis, GPC chromatogram, rheological analysis and thermal analyses (DSC and TGA) of SH(PCI). ¹H-NMR spectra of the reactive diluents. Evaluation of the biobased content of photocurable mixtures. Evaluation of printing performances. Tensile stress-strain curves of 3D-printed materials.

ACKNOWLEDGMENTS

This work was funded the Project Ecosyster - Ecosystem for Sustainable Transition in Emilia-Romagna, grant number ECS00000033, within Spoke 1 activities (Materials for sustainability and ecological transition, CUP J33C22001240001).

AUTHOR INFORMATION

Corresponding Authors

*Mirko Maturi, Department of Industrial Chemistry “Toso Montanari”, University of Bologna. Via P. Gobetti 85, 40129 Bologna (Italy). Email: mirko.maturi2@unibo.it

*Mauro Comes Franchini, Department of Industrial Chemistry “Toso Montanari”, University of Bologna. Via P. Gobetti 85, 40129 Bologna (Italy). Email: mauro.comesfranchini@unibo.it

Present Addresses

† Mirko Maturi, Departamento de Ciencia de los Materiales e Ing. Metalúrgica y Química Inorgánica (IMEYMAT), Universidad de Cádiz, Avda. República Saharaui, s/n 11510 Puerto Real (Spain). Email: mirko.maturi@uca.es

Author Contributions

The manuscript was written through contributions of all authors. All authors have given approval to the final version of the manuscript.

REFERENCES

- (1) Attaran, M. The Rise of 3-D Printing: The Advantages of Additive Manufacturing over Traditional Manufacturing. *Bus. Horiz.* **2017**, *60* (5), 677–688.

<https://doi.org/10.1016/j.bushor.2017.05.011>.

- (2) Voet, V. S. D.; Guit, J.; Loos, K. Sustainable Photopolymers in 3D Printing: A Review on Biobased, Biodegradable, and Recyclable Alternatives. *Macromol. Rapid Commun.* **2021**, *42* (3), 2000475. <https://doi.org/10.1002/marc.202000475>.
- (3) Shahrubudin, N.; Lee, T. C.; Ramlan, R. An Overview on 3D Printing Technology: Technological, Materials, and Applications. *Procedia Manuf.* **2019**, *35*, 1286–1296. <https://doi.org/10.1016/j.promfg.2019.06.089>.
- (4) Maines, E. M.; Porwal, M. K.; Ellison, C. J.; Reineke, T. M. Sustainable Advances in SLA/DLP 3D Printing Materials and Processes. *Green Chem.* **2021**, *23* (18), 6863–6897. <https://doi.org/10.1039/D1GC01489G>.
- (5) Werpy, T.; Petersen, G. Top Value Added Chemicals from Biomass: Volume I -- Results of Screening for Potential Candidates from Sugars and Synthesis Gas. *Us Nrel* **2004**, Medium: ED; Size: 76 pp. pages. <https://doi.org/10.2172/15008859>.
- (6) Willke, T.; Vorlop, K. D. Biotechnological Production of Itaconic Acid. *Appl. Microbiol. Biotechnol.* **2001**, *56* (3–4), 289–295. <https://doi.org/10.1007/s002530100685>.
- (7) Zhang, R.; Liu, H.; Ning, Y.; Yu, Y.; Deng, L.; Wang, F. Recent Advances on the Production of Itaconic Acid via the Fermentation and Metabolic Engineering. *Fermentation* **2023**, *9* (1), 71. <https://doi.org/10.3390/fermentation9010071>.

- (8) Maturi, M.; Pulignani, C.; Locatelli, E.; Vetri Buratti, V.; Tortorella, S.; Sambri, L.; Comes Franchini, M. Phosphorescent Bio-Based Resin for Digital Light Processing (DLP) 3D-Printing. *Green Chem.* **2020**, *22* (18), 6212–6224. <https://doi.org/10.1039/D0GC01983F>.
- (9) Vetri Buratti, V.; Sanz de Leon, A.; Maturi, M.; Sambri, L.; Molina, S. I.; Comes Franchini, M. Itaconic-Acid-Based Sustainable Poly(Ester Amide) Resin for Stereolithography. *Macromolecules* **2022**, *55* (8), 3087–3095. <https://doi.org/10.1021/acs.macromol.1c02525>.
- (10) Pérocheau Arnaud, S.; Malitowski, N. M.; Meza Casamayor, K.; Robert, T. Itaconic Acid-Based Reactive Diluents for Renewable and Acrylate-Free UV-Curing Additive Manufacturing Materials. *ACS Sustain. Chem. Eng.* **2021**, *9* (50), 17142–17151. <https://doi.org/10.1021/acssuschemeng.1c06713>.
- (11) Maturi, M.; Spanu, C.; Maccaferri, E.; Locatelli, E.; Benelli, T.; Mazzocchetti, L.; Sambri, L.; Giorgini, L.; Comes Franchini, M. (Meth)Acrylate-Free Three-Dimensional Printing of Bio-Derived Photocurable Resins with Terpene- and Itaconic Acid-Derived Poly(Ester-Thioether)S. *ACS Sustain. Chem. Eng.* **2023**, *11* (49), 17285–17298. <https://doi.org/10.1021/acssuschemeng.3c04576>.
- (12) Chiulan, I.; Frone, A.; Brandabur, C.; Panaitescu, D. Recent Advances in 3D Printing of Aliphatic Polyesters. *Bioengineering* **2017**, *5* (1), 2.

<https://doi.org/10.3390/bioengineering5010002>.

- (13) Gunatillake, P.; Adhikari, R. Biodegradable Synthetic Polymers for Tissue Engineering. *Eur. Cells Mater.* **2003**, *5*, 1–16. <https://doi.org/10.22203/eCM.v005a01>.
- (14) Caretto, A.; Noè, M.; Selva, M.; Perosa, A. Upgrading of Biobased Lactones with Dialkylcarbonates. *ACS Sustain. Chem. Eng.* **2014**, *2* (9), 2131–2141. <https://doi.org/10.1021/sc500323a>.
- (15) Thomas, S. M.; DiCosimo, R.; Nagarajan, V. Biocatalysis: Applications and Potentials for the Chemical Industry. *Trends Biotechnol.* **2002**, *20* (6), 238–242. [https://doi.org/10.1016/S0167-7799\(02\)01935-2](https://doi.org/10.1016/S0167-7799(02)01935-2).
- (16) Baheti, P.; Gimello, O.; Bouilhac, C.; Lacroix-Desmazes, P.; Howdle, S. M. Sustainable Synthesis and Precise Characterisation of Bio-Based Star Polycaprolactone Synthesised with a Metal Catalyst and with Lipase. *Polym. Chem.* **2018**, *9* (47), 5594–5607. <https://doi.org/10.1039/C8PY01266K>.
- (17) Elomaa, L.; Teixeira, S.; Hakala, R.; Korhonen, H.; Grijpma, D. W.; Seppälä, J. V. Preparation of Poly(ϵ -Caprolactone)-Based Tissue Engineering Scaffolds by Stereolithography. *Acta Biomater.* **2011**, *7* (11), 3850–3856. <https://doi.org/10.1016/j.actbio.2011.06.039>.
- (18) Asikainen, S.; van Bochove, B.; Seppälä, J. V. Drug-Releasing Biopolymeric Structures Manufactured via Stereolithography. *Biomed. Phys. Eng. Express* **2019**, *5* (2), 025008.

<https://doi.org/10.1088/2057-1976/aaf0e0>.

- (19) Arif, Z. U.; Khalid, M. Y.; Noroozi, R.; Sadeghianmaryan, A.; Jalalvand, M.; Hossain, M. Recent Advances in 3D-Printed Polylactide and Polycaprolactone-Based Biomaterials for Tissue Engineering Applications. *Int. J. Biol. Macromol.* **2022**, *218*, 930–968. <https://doi.org/10.1016/j.ijbiomac.2022.07.140>.
- (20) Lang, M.; Wong, R. P.; Chu, C.-C. Synthesis and Structural Analysis of Functionalized Poly (ϵ -Caprolactone)-Based Three-Arm Star Polymers. *J. Polym. Sci. Part A Polym. Chem.* **2002**, *40*(8), 1127–1141. <https://doi.org/10.1002/pola.10171>.
- (21) Doganci, M. D. Effects of Star-Shaped PCL Having Different Numbers of Arms on the Mechanical, Morphological, and Thermal Properties of PLA/PCL Blends. *J. Polym. Res.* **2021**, *28*(1), 11. <https://doi.org/10.1007/s10965-020-02380-2>.
- (22) Chakrabarty, K.; Forzato, C.; Nitti, P.; Pitacco, G.; Valentin, E. The First Kinetic Enzymatic Resolution of Methyl Ester of C75. *Lett. Org. Chem.* **2010**, *7*(3), 245–248. <https://doi.org/10.2174/157017810791112405>.
- (23) Delolo, F. G.; dos Santos, E. N.; Gusevskaya, E. V. Anisole: A Further Step to Sustainable Hydroformylation. *Green Chem.* **2019**, *21* (5), 1091–1098. <https://doi.org/10.1039/C8GC03750G>.
- (24) Żółtowska, K.; Sobczak, M.; Olędzka, E. Novel Zinc-Catalytic Systems for Ring-Opening Polymerization of ϵ -Caprolactone. *Molecules* **2015**, *20* (2), 2816–2827.

<https://doi.org/10.3390/molecules20022816>.

- (25) Gaborieau, M.; Castignolles, P. Size-Exclusion Chromatography (SEC) of Branched Polymers and Polysaccharides. *Anal. Bioanal. Chem.* **2011**, *399* (4), 1413–1423. <https://doi.org/10.1007/s00216-010-4221-7>.
- (26) An, S. G.; Cho, C. G. Synthesis and Characterization of Amphiphilic Poly(Caprolactone) Star Block Copolymers. *Macromol. Rapid Commun.* **2004**, *25* (5), 618–622. <https://doi.org/10.1002/marc.200300118>.
- (27) Lemmouchi, Y.; Perry, M. C.; Amass, A. J.; Chakraborty, K.; Schacht, E. Novel Synthesis of Biodegradable Amphiphilic Linear and Star Block Copolymers Based on Poly(ϵ -caprolactone) and Poly(Ethylene Glycol). *J. Polym. Sci. Part A Polym. Chem.* **2007**, *45* (17), 3975–3985. <https://doi.org/10.1002/pola.22151>.
- (28) Ouyang, Q.; Cheng, L.; Wang, H.; Li, K. Mechanism and Kinetics of the Stabilization Reactions of Itaconic Acid-Modified Polyacrylonitrile. *Polym. Degrad. Stab.* **2008**, *93* (8), 1415–1421. <https://doi.org/10.1016/j.polymdegradstab.2008.05.021>.
- (29) Loginova, E. V.; Mikheev, I. V.; Volkov, D. S.; Proskurnin, M. A. Quantification of Copolymer Composition (Methyl Acrylate and Itaconic Acid) in Polyacrylonitrile Carbon-Fiber Precursors by FTIR-Spectroscopy. *Anal. Methods* **2016**, *8* (2), 371–380. <https://doi.org/10.1039/C5AY02264A>.
- (30) Zhu, Y.; Yang, J.; Mei, F.; Li, X.; Zhao, C. Bio-Based 1,4-Butanediol and Tetrahydrofuran

- Synthesis: Perspective. *Green Chem.* **2022**, *24* (17), 6450–6466.
<https://doi.org/10.1039/D2GC02271K>.
- (31) Xiang, J.; Yang, S.; Zhang, J.; Wu, J.; Shao, Y.; Wang, Z.; Yang, M. The Preparation of Sorbitol and Its Application in Polyurethane: A Review. *Polym. Bull.* **2022**, *79*(4), 2667–2684. <https://doi.org/10.1007/s00289-021-03639-4>.
- (32) Hsieh, S.-C.; Wang, J.-H.; Lai, Y.-C.; Su, C.-Y.; Lee, K.-T. Production of 1-Dodecanol, 1-Tetradecanol, and 1,12-Dodecanediol through Whole-Cell Biotransformation in *Escherichia Coli*. *Appl. Environ. Microbiol.* **2018**, *84* (4).
<https://doi.org/10.1128/AEM.01806-17>.
- (33) Rodiansono; Dewi, H. P.; Mustikasari, K.; Astuti, M. D.; Husain, S.; Sutomo. Selective Hydroconversion of Coconut Oil-Derived Lauric Acid to Alcohol and Aliphatic Alkane over MoO_x-Modified Ru Catalysts under Mild Conditions. *RSC Adv.* **2022**, *12* (21), 13319–13329. <https://doi.org/10.1039/D2RA02103J>.
- (34) Mondschein, R. J.; Kanitkar, A.; Williams, C. B.; Verbridge, S. S.; Long, T. E. Polymer Structure-Property Requirements for Stereolithographic 3D Printing of Soft Tissue Engineering Scaffolds. *Biomaterials* **2017**, *140*, 170–188.
<https://doi.org/10.1016/j.biomaterials.2017.06.005>.
- (35) Maturi, M.; Comes Franchini, M. Composizione Fotoreticolabile e Suoi Componenti Da Fonti Di Origine Rinnovabile, per Processi Di Stampa Tridimensionale.

PCT/IB2022/061255.